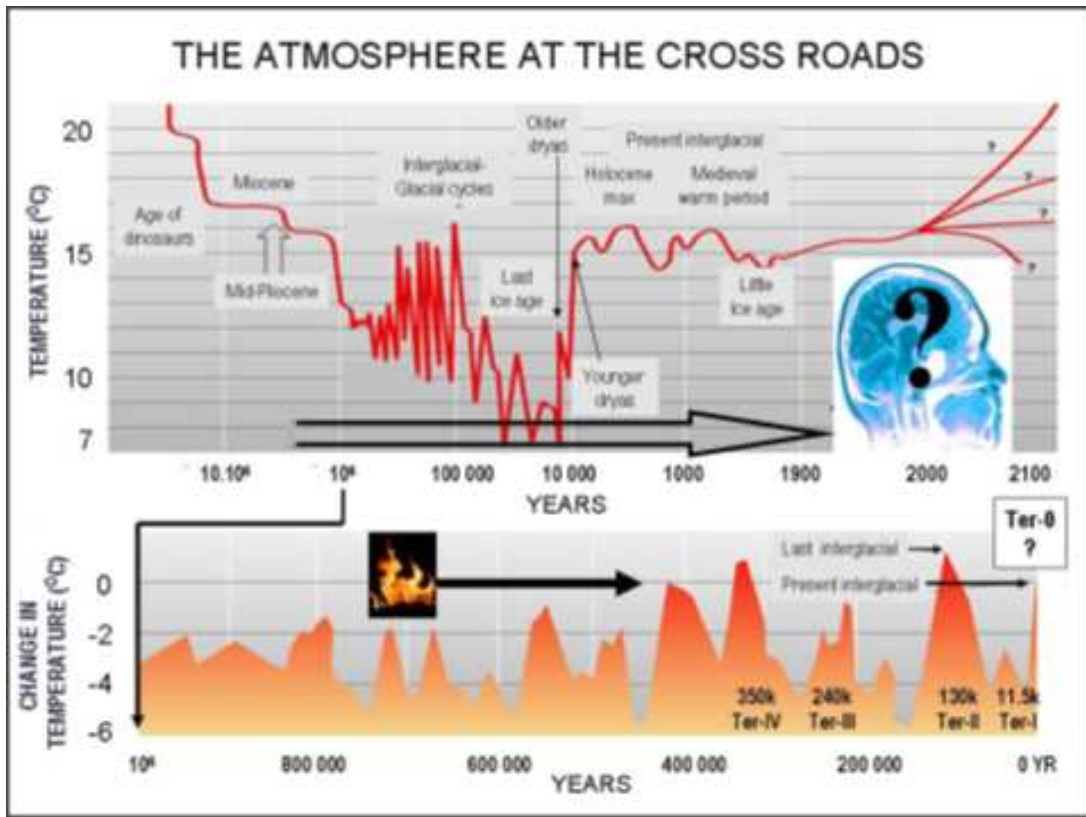


Trends and tipping point in the climate system: portents for the 21st century

Andrew Glikson
Earth and Palaeoclimate science
Australian National University

Mass extinctions in the history of Earth occurred when the atmosphere-ocean-land carbon and oxygen cycles, on which the biosphere depends, have been perturbed at rates to which species could not adapt. Rising atmospheric greenhouse gas levels above 330 ppm CO₂ at rates of ~2 ppm/year and mean temperature rise of ~0.016°C/year since 1975-1976 are driving the fastest climate change trend recorded since about 34 million years ago, representing a critical climate threshold leading into uncharted territory and threatening the biosphere and human civilization. It is suggested the arrest of carbon emissions may not be sufficient to halt the current trend, except if accompanied with global efforts at down-draw of atmospheric CO₂ using a range of bio-sequestration, organic and chemical methods.

- I. Synopsis
- II. Pre-Holocene atmospheres
- III. The Holocene
- IV. The Anthropocene
- V. Extreme weather events and tipping points
- VI. 20-21st centuries' climate projections
- VII. CO₂ draw-down
- VIII. 2011 climate developments



I. Synopsis

This paper examines deep-time perspectives of 20th to early 21st centuries trends in the atmosphere-ocean system with reference to future climate change projections. Mass extinctions in the history of Earth occurred when the atmospheric carbon and oxygen cycles, constituting the 'lungs' on which the biosphere depends, were perturbed at rates to which species could not adapt. By contrast to linear mean global temperature trends in the range of +1.8 to +3.6°C projected by the IPCC AR4¹, the glacial-interglacial history of the last ~800 kyr (1 kyr = 1000 years) is dominated by non-linear trends, stochastic (probability-related) events and abrupt climate shifts, including irreversible tipping points driven by orbital forcing and GHG (greenhouse gas) feedbacks, as well as perturbed by short-term volcanic events. During glacial-interglacial cycles the atmosphere-ocean-cryosphere system responded to significant radiative forcing (energy drivers) which triggered amplifying feedbacks driving irreversible shifts between relatively stable climate states. Ice core evidence for abrupt climate changes during the upper Pleistocene include (1) During 75–20 kyr ~1470 years-long intra-glacial cycles (Dansgaard-Oeschger and Heinrich events) involved abrupt warming in Greenland, extending to the tropics, where temperature rises occurred at rates of ~6–8°C and <3°C, respectively, over a few decades, attributed to periodic ice melting events²; (2) The onset and termination of the 12.9–11.7 kyr *Youngest dryas* cold phase in Greenland over periods as short as 1–3 years. Whereas these events were driven mainly by ice melt/open water albedo-flip feedbacks, related GHG rise rates were less than at present. Glacial termination events were preceded by low-variability lulls. By contrast, temperature rise rates during 1880–2009 and 1975–2009 exceed those of the last glacial termination by factors of ~10 and ~26, respectively (Table 1). The current GHG rise at ~2 ppm CO₂/year is the fastest observed in the geological record, with the exception of events associated with mass extinction of species. This rate is higher by a factor of ~5 than that associated with the Palaeocene-Eocene thermal event (PETM) when a release of ~2000 billion ton carbon (GtC) triggered an abrupt greenhouse event of ~ +5°C (deep ocean temperature) within few decades, and which lasted up to 10,000 years³. The current GHG forcing level of +3.2 Watt/m² since 1750 AD⁴, driven by carbon emission, fires and land clearing and masked by sulphur aerosol albedo enhancement estimated as -1.6 Watt/m², has reached near-50 per cent of the ~6 Watt/m² forcing value of the last glacial termination. At 392 ppm CO₂ and 470 ppm CO₂-equivalent, the atmosphere/ocean system is just below the CO₂ 500±50 ppm upper stability limit of the Antarctic ice sheet. Ocean-induced lag effects modelled as a climate response function by Hansen et al. 2011 constitutes an added factor. Rising GHG level will, in part, buffer the atmosphere in relation to solar orbital forcing, induce a near-permanent El-Nino state analogous to conditions of the Pliocene and mid-Miocene, when mean global temperatures were +2 to +4°C above present, continental ice sheets near half the present and sea levels ~ +20 to 40 meters above present. Since 1975–1976 rising atmospheric GHG above 350 ppm CO₂ and mean temperatures at ~0.016°C/year are driving the fastest climate change trend recorded since ~34 million years (Ma) ago, representing a critical threshold leading the climate into uncharted territory and threatening the Holocene biosphere. Depending on the level of future GHG rise, elevated temperatures would delay or cancel the next glacial cycle. The extended super-heated interglacial is leading toward a mass extinction of species analogous to some of the more extreme in terrestrial history.

¹ IPCC AR4 2007.

² Ganopolski . and Rahmstorf, 2001. Physical Review Letters 88, 3. 038501 (1-4)

³ Zachos et al. 2008. Nature, Vol 451, p 279–283

⁴ Hansen et al., 2011. www.columbia.edu/~jeh1/.../20110415_EnergyImbalancePaper.pdf

Table 1.

Comparison of mean global temperature rise rates during Pleistocene glacial terminations, Dansgaard-Oeschger intra-glacial cycles and 20-21st century

Reference	Period	T°C	T°C/year	
	1975-2009	+0.56	~0.016	NASA/GISS
	1880-2009	+0.8	~0.0062	NASA/GISS
Last glacial termination	16 – 10 kyr 14 - 10 kyr	~ +4.5 ~ +2.5	~0.00075 ~0.0006	(Petit et al., 1999) ⁵
Dansgaard-Oeschger events (21 cycles) Av cycle ~1540 years	~80 years	~ +6	~0.075	
Termination-II (Eemian)	8 kyr	~ +5	~0.00062	Petit et al., 1999
Termination-III	5 kyr	~ +5	~0.001	Petit et al., 1999
Termination IV	12 kyr	~ +5	~0.0004	Petit et al., 1999

II. Pre-Holocene atmospheres

Excepting relatively short ice ages and cold stages the history the atmosphere-ocean system has been dominated by greenhouse gas (GHG)-rich conditions, inducing warm and acid (low-pH) oceans—consequent on accumulation of CO₂ and methane emitted by volcanic activity, through metamorphism, asteroid impacts and emanation from methane deposits. Low levels of CO₂ sequestration by warm low-pH oceans led to a build-up of atmospheric CO₂ to several thousand parts per million (ppm) CO₂ during much of the Palaeozoic and Mesozoic (Fig. 1)⁶. These conditions were interrupted by ice ages, including the late Ordovician glaciation (c.446-443 Ma) (1 Ma: 1 million years-ago), Carboniferous-Permian glaciation (c.300–270 Ma), minor Jurassic cold periods and post-Eocene glaciation from 34 Ma (Fig. 1). During the glacial periods strong CO₂-sequestration by weathering and erosion of mountain ranges (combination of released Ca with CO₂)⁷, sequestration by plant photosynthesis and burial of carbonaceous shale and coal resulted in low atmospheric CO₂, exposing the Earth to the effects of solar radiation (orbital forcing) represented by the Milankovic glacial-interglacial cycles⁸.

The emergence of land plants in the late Silurian (~420 Ma), the earliest being vascular plants (*Cooksonia*, *Baragwanathia*), and later Cycads and Ginkgo in the Permian (299–251 Ma), combined with the rise in photosynthetic oxygen above 13% (Fig. 1), set the stage for land fires, coating many parts of the land with a thin layer of carbon, including cellulose in trees, grasses, soils and bogs, and as methane hydrate and methane clathrate deposits in bogs, sediments and

⁵ Petit et al. 1999. *Nature* 399, 3 June 429-436 |www.nature.com

⁶ Zachos et al., 2001. *Science*, Vol 292, p 686–693; Glikson, 2008. *Aust. Journal Australia Earth Science*, 55, 125-140.

⁷ Ruddiman, 1997. *Tectonic Uplift and Climate Change*, Springer, 1997, ISBN 978-0-306-45642-8

⁸ Royer et al., 2004. *GSA Today*, 14, 4-10; Royer et al., 2007. *Nature*, 446. Beerling and Berner, 2005. *Proceedings National Academy Science* 102, 1302-1305; Berner, 2004. Oxford University Press, New York; Berner, 2006. *Geochimica et Cosmochimica Acta* 70, 5653–5664; Berner et al., 2007. *Science* 316, 557-558.

permafrost⁹. The carbon, when combined with oxygen emitted through photosynthesis, ensued in flammable land surfaces, repeatedly ignited by lightning and volcanic eruptions. Burial of carbon in sediments has stored the fuel over geological periods, buffering the surface inventory of combustible material—pending the arrival of the genus Homo¹⁰.

Following a release of some 2000 Gigaton carbon (1 GtC: 1 billion ton) as methane 55 Ma-ago, elevating atmospheric CO₂ to near-3000 ppm and mean temperatures by ~5°C¹¹, a gradual decline in mean global CO₂ and temperatures culminated in the end-Eocene (34 Ma) with a sharp drop below 500 ppm CO₂ and several degrees C, driving the onset of the Antarctic ice sheet (Fig. 2). Whereas upper Eocene temperature decline is attributable to CO₂ capture associated with erosion of the rising Himalayan and Alpine mountain chains¹², their sharp fall at 34 Ma can be attributed to the opening of the Drake Passage between South America and west Antarctica, ensuing in the circum-Antarctic cold current and isolation of Antarctica from the influence of warmer currents. The transition was preceded by a large cluster of end-Eocene asteroids (Popigai, Chesapeake Bay, Timor Sea impacts) whose atmospheric dusting effects may have enhanced the fall of temperature¹³.

Studies of the glacial-interglacial era post-34 Ma to the present based on proxies of temperature (cf. oxygen isotopes, Ca/Mg ratios), greenhouse gases (fossil plant pores/stomata), wind (dust content in marine sediments), salinity (boron) and biological activity (pollen, organic remains of algae [alkenones], plant wax residues in sediments) allow detailed knowledge of this era¹⁴. The upper Eocene cooling and following ice ages saw the flourishing of mammals, which in the Mesozoic were restricted to small burrowing species. The glacial state since 34 Ma was interrupted by short warming events accompanied with sea level rises, including the late Oligocene (25 Ma), early and mid-Miocene (17-14 Ma) and late-Pliocene (3.1–2.9 Ma) (Fig. 2).

Changes in ocean currents related to the rise of the Panama Cordillera and thereby isolation of the Pacific and Atlantic oceans ~4 Ma-ago augmented cross-latitude ocean circulation, enhancing the Pacific Gyre, the El Niño Southern Oscillation (ENSO) cycle¹⁵ and the North Atlantic Thermohaline Current (NATH). The decline in atmospheric greenhouse gas concentrations (from ~400 ppm), of temperatures (by at least 2°C) and sea levels (by ~25 meters) during the transition from ~2.8 Ma removed part of the GHG buffer, exposing the surface to the effects of the Milankovic glacial-interglacial cycles, including precession (axial rotation), axial obliquity and orbital eccentricity, controlling the Earth-sun relations. The cooling saw the formation of the Greenland, Laurentian and Scandinavian ice sheets and established open savannah African environment where Hominids developed. The decrease in CO₂ levels enhanced the effect of ~100 kyr (1 kyr = thousand years) eccentricity-dominated cycles, with CO₂

⁹ Bowman, D.M. et al., 2009. Fire in the Earth system. *Science*, 24 (324): 481-484

¹⁰ Glasspool et al., 2004. *Geology*, 32: 381-383; Keeley and Rundel, 2005. *Ecology Letters*, 7: 683–690.

¹¹ Zachos et al., 2008. *Nature*, Vol 451, p 279–283

¹² Ruddiman et al., 1997. In: *Tectonic Uplift and Climate Change*, (W.F. Ruddiman, Ed.), Plenum, NY. pp. 471-515.

¹³ Glikson, 2005. *Earth and Planetary Science Letters*, 236: 933-937.; Glikson et al., 2010. *Australian Journal of Earth Sciences* (2010) 57, 411-430.

¹⁴ Royer et al., 2004. *GSA Today*, 14, 4-10; Royer, 2006. *Geochimica et Cosmochimica Acta*, 70, 5665–5675.

¹⁵ Fedorov et al., 2006. *Science* 9, 312 no. 5779, 1485-1489

fluctuations of 180 to 280 ppm, temperature shifts of $\pm 5^{\circ}\text{C}$ and sea levels of $\pm \sim 100$ meter (Fig. 3).

The Pliocene-Pleistocene transition from tropical to savannah environments in Africa, accompanied with faunal changes from tropical to arid-zone type species, including abrupt diversifications of antelopes at ~ 2.8 , 1.8-1.7 and 0.8-0.7 Ma¹⁶, signifies an increase in climate variability and an enhanced pace of evolution. Human evolution accords with these transitions in terms of variability selection, diversification and appearance of Olduvan stone tools from ~ 2.7 Ma and Acheulean stone tools from ~ 1.7 Ma.

The temporal increase in intensity of glacial-interglacial polarities and the abrupt nature of the glacial terminations are attributed to solar pulsations maxima of 40-60 Watt/m² in northern upper mid-latitudes, which in turn trigger powerful feedback effects related to:

1. The ice melt albedo-flip process, where the albedo loss of melting ice, the infrared absorption by melt water and spreading vegetation result in self-amplifying feedback processes.
2. Release of CO₂ from warming oceans and drying biosphere, warming the atmosphere and leading to further CO₂ release in a feedback cycle. These greenhouse gas cycles typically followed the onset of ice melt albedo-flip cycles by ~ 800 years.

The glacial termination of 14.7-11.7 kyr (thousand years ago), culminating in the transient '*Younger dryas*' cool phase (12.9-11.7 kyr) was followed at c.8.2 kyr by the so-called '*Holocene Optimum*', involving rapid melting of the Fennoscandian and Greenland ice sheets and thereby cooling of the North Atlantic by several degrees Celsius.

III. Holocene

A gradual to protracted cooling trend through the Holocene interglacial from ~ 8.2 kyr to the 18th century was interrupted by mild warming phase ~ 900 -1400 AD years-ago (MWP - Medieval Warm Period - MWP) and a protracted cool phase peaking at c.1550 - 1800 AD (LIA - Little Ice Age) (Fig. 4). Broadly these periods corresponded to solar insolation high up to +0.5 watt/m² and minimum of -0.5 watt/m², respectively (Fig. 4). Other factors may include a rise in vegetation cover associated with decline in cultivation during the MWP, which led to an increase in CO₂ sequestration and thus to cooling leading to the LIA.

A decline in CO₂ and methane from the *Holocene Optimum* ~ 9.0 -8.0 kyr ago was replaced by a slow rise in CO₂ from ~ 6000 BC and methane from ~ 4000 BC (Fig. 5), attributed to land clearing, wheat and rice cultivation and fires, slowed down the overall cooling toward the next ice age. According to Ruddiman¹⁷ the natural interglacial cycle has been interrupted by Neolithic burning and land clearing, halting a decline in CO₂ and methane and thereby onset of the next glacial. Other authors regard the mid-Holocene rise in greenhouse gases as a natural trend comparable with the 420-405 kyr Holsteinian interglacial¹⁸.

¹⁶ deMenocal, 2004. Earth and Planetary Science Letters, Vol 220, p 3-24.

¹⁷ Ruddiman, W.F, 2003. Quaternary Science reviews, 22, 1597-1629.

¹⁸ Broecker and Stocker, 2006. Eos 87(3): 27-29.

IV. Anthropocene

Since the 18th century burning of fossil fuels has released some **352** GtC (billion ton carbon), whereas land clearing resulted in an increase of **152** GtC to the atmosphere¹⁹, the latter due to decline in photosynthesis and depletion of soil carbon contents, the total being close to the original carbon budget of the atmosphere **~590** GtC. Of the additional CO₂ approximately 42 per cent stays in the atmosphere (Fig. 6). Combined with other greenhouse gases this led to an increase in atmospheric energy level of ~ 3.2 Watt/m² and (for climate sensitivity of 3°C per doubling of CO₂) a rise of potential mean global temperature by +2.3°C²⁰ (Fig. 7). Approximately -1.6 Watt/m², equated with -1.1°C, is masked by emitted sulphur aerosols. Consequently measured mean global temperature rise reached $\sim 0.8^\circ\text{C}$ since 1800 AD (Fig. 8a, b) whereas polar temperatures have reached above +4°C (Fig. 9) – representing the effects of the ice melt albedo flip process. Since 1975-1976 a decline in the emission of sulphur aerosols and their albedo effects resulted in a sharp increase in temperature (Fig. 8a). Since 2002 the Greenland and Antarctica ice sheets have been melting at rates which double every 5-10 years (Fig. 10), having become the major contributors to sea levels which since 1992 rose by $\sim 3.0 \pm 0.4$ mm/year (Fig. 11).

Based on palaeoclimate studies, the current levels of CO₂ of 392 ppm²¹ and of CO₂-equivalent of above 455 ppm²², a value which includes the effects of methane and nitrous oxide, commit the atmosphere to a warming trend which, if continued, will lead toward an ice-free Earth conditions.

By the onset of the 3rd millennium the release to the atmosphere and oceans of more than 500 GtC from fossil biospheres, proceeding at a rate of ~ 2 ppm/year, a rate unprecedented in recorded geological history. An exception is the release to the atmosphere of some 2000 billion tons carbon at the Paleocene–Eocene boundary at 55 Ma, estimated to have raised atmospheric CO₂ levels at a rate of about 0.4 ppm/year, with an attendant extinction event. Other exceptions are volcanic eruptions and asteroid impacts which have ignited regional to global wildfires and, in the case of impacts, excavated and vaporized carbon-rich sediments.

Since the 1980s global temperature, ice melt rates and sea level rise have been lagging behind rising atmospheric energy levels (Fig. 7). With ensuing desertification of temperate zones, e.g. southern Europe, south and southwest Australia and southern Africa, forests become prey to firestorms. According to Bowman et al. (2009)²³ carbon emissions from natural and human-lit fires have reached 2 - 4 GtC/year. The rise in CO₂ ensues in powerful amplifying feedbacks, including sea and land ice melt decreasing the Earth's albedo and increasing the area of exposed water, absorption of infrared and warming.

Warming of the oceans leads to a decrease in CO₂ sequestration and to increased acidity. Increased evaporation in warming oceans leads to an enhanced hydrological cycle, including abrupt precipitation events, floods and intensified cyclones. At ~ 455 ppm CO₂-equivalent the climate is tracking just under the upper stability limit of the Antarctic ice sheet, defined at approximately 500 ± 50 ppm.

¹⁹ Global Carbon Project

²⁰ Hansen et al., 2011. www.columbia.edu/~jeh1/.../20110415_EnergyImbalancePaper.pdf

²¹ Mouna Loa CO₂ <http://www.esrl.noaa.gov/gmd/ccgg/trends/>

²² IPCC-2007 AR4 WG3 Chapter 1

²³ Bowman et al., 2009. Science, 24 (324): 481-484

The first decade of the 21st century has been the warmest in the instrumental record (Fig. 8 inset). Current trends shift the state of the atmosphere to conditions analogous to those of the end Pliocene ~2.8 Ma-ago (Fig. 3), a period when the bulk of the Greenland and west Antarctic ice sheets melted. Current melting of these ice sheets, consequent on high temperature rise in polar regions (Fig. 9), is doubling every 5 to 10 years (Fig. 10), exceeding the contribution to sea level rise from thermal expansion and mountain glaciers. Since 2005 the Greenland and Antarctica ice mass was reduced by ~1000 and ~700 Gigaton ice. The rise of CO₂-equivalent above 500 ppm and mean global temperatures above +4°C would track toward greenhouse Earth conditions such as existed during the early Eocene some 50 million years ago.

Sea level rise represents the sum-total of climate change processes, including thermal expansion of water, melting ice sheets and mountain glaciers. Since the early 20th century, the rate of sea level rise increased from ~1 mm/year, the 1992–2010 rate being 3.0+/-0.4 mm/year (Fig. 11).

Climate change is expressed by a shift of mid-latitude high pressure ridges and climate zones toward the poles. The increase in ocean-land energy levels has led to intensification of the hydrological cycle, floods, cyclones and heat waves, which have increased by a factor of two to three since 1980 (Fig. 12). In geological terms human-induced climate change constitutes a global oxygenation of both the present biosphere and the fossil remains of ancient biospheres, exceeding any recorded since 55 Ma-ago.

V. Extreme weather events and tipping points

At 392 ppm CO₂ atmospheric CO₂ levels are ~110 ppm higher than the maximum of ~280 ppm of interglacial phases since 800 kyr, with global warming effects currently mitigated by the cooling effect of albedo-enhancing sulphur aerosols (~ -1.6 Watt/m² = ~ -1.2°C), which act as an (unintended) global geo-engineering measure (Fig. 7). Further lag effects are induced by the buffering effects of the oceans, modelled as a response function by Hansen et al. (2011). Without this short-lived (~3 years long) cooling effect the internationally agreed maximum temperature target of <2°C has been transcended.

The 0.2–1.0°C rise in sea surface temperature over large parts of the tropical and subtropical oceans during 1800–2011 relative to 1951–1980²⁴ resulted in an enhanced hydrological evaporation/precipitation cycle, ensuing in cyclones and floods, while the rise in land temperatures leads to heat waves and fires. Accordingly the frequency of extreme weather events has increased by 2 to 3 fold during 1980 – 2008 (Fig. 12). In the case of cyclones an increase in intensity is not everywhere accompanied by an increase in frequency. Rahmstorf and Coumou (2011)²⁵ conducted a statistical analysis of the relations between long term climate trends and the incidence of extreme weather events, finding that the number of record-breaking heat events increases approximately in proportion to the ratio of warming trend to short-term standard deviation (variability). Short-term variability decreases the number of heat extremes, whereas a (longer term) climatic warming increases it.

Lenton et al. (2008)²⁶ indicate multiple potential tipping points in the Earth system, including melting and instability of the Greenland and west Antarctic ice

²⁴ <http://data.giss.nasa.gov/gistemp/maps/>

²⁵ Rahmstorf, S.R. and Coumou, D., 2011. PNAS. www.pnas.org/cgi/doi/10.1073/pnas.1101766108

²⁶ Lenton, T.M. et al., 2008. PNAS, 105, 1786–1793

sheets (much of the latter grounded below sea level), melting of permafrost, Boreal forest dieback and tundra loss, Indian and west African monsoon shifts, Amazon forest dieback, ozone hole growth and changes to the ENSO circulation and ocean deep water formation patterns (Fig. 13).

Emissions of both CO₂ and sulphur emissions have grown during WWI and WWII, accelerating from about 1950 in connection with the post-war economic boom (Fig. 8c). A mean global temperature lull and a degree of cooling during 1940-1975, related to rising levels of sulphur aerosols (Fig. 8c) and a low in the 11-years sun spot cycle (Fig. 8b), were terminated with an abrupt warming trend in ~1975 when atmospheric CO₂ level reached ~330 ppm and clear air policies reduced sulphur emissions (Fig. 8b). Hansen et al. (2008) regard a CO₂ level of ~350 ppm as the maximum allowable before amplified feedbacks lead to tipping points beyond human control.

Following the 1998 peak El Nino event (Fig. 8a. inset) the overall temperature rise rate declined relative to the 1975-1998 period, accounted in part due to the resumption of SO₂ rise (Fig. 8c) and a decline in sunspot activity (Fig. 8b). Despite of these factors mean temperatures of the 1st decade of the 21st century are the highest in the instrumental record.

The definition of *tipping point* refers to the onset of irreversible change of global climate between stable states or, according to Lenton et al. 2008, the critical threshold at which a tiny perturbation can qualitatively alter the state of a system. Runaway climate change occurs when the climate system transgresses a point beyond which amplifying positive feedback effects drive further climate change until negative feedbacks, such as significant decrease in solar insolation, stabilize a new climate state. According to James Hansen this point has already been reached with carbon dioxide levels currently at 392 ppm, stating: "*Further global warming of 1°C defines a critical threshold. Beyond that we will likely see changes that make Earth a different planet than the one we know*"²⁷.

Such a positive feedback is the opening of the Arctic Sea, which allows the absorption of as much solar energy as that added by emitted atmospheric CO₂²⁸. Melting of Arctic ice leading to increased evaporation can result in the advance of cold fronts leading to snow storms in the north Atlantic and north Pacific, as occurred recently²⁹. Further positive feedbacks occur due to the release of methane deposits, including from Arctic permafrost (~900 GtC), high-latitude peat lands (~400 GtC), Tropical peat lands (~100 GtC) and vegetation subject to fire and/or deforestation³⁰. Lovelock suggests the climate has already crossed the tipping point into a permanently hot state some 5°C higher than Holocene pre-industrial levels³¹.

The early Holocene climate record contains examples for cooling triggered by ice melt influx into the North Atlantic Ocean, including (1) during the 12.9-11.7 kyr *Youngest dryas* interval and (2) following the Holocene Optimum at ~8.2 kyr, consequent on the collapse of the Laurentian ice sheet and cold ice melt water influx through Lake Agassiz. This raises a question whether the relative cooling of some ocean regions, including parts of the North Pacific, North Atlantic and

²⁷ <http://afp.google.com/article/ALeqM5g2Wkbo6PcynAVEJzSPWDQZaWAI8g>

²⁸ <http://www.dazeddigital.com/artsandculture/article/3703/1/vivienne-westwood-meets-james-lovelock-on-video>

²⁹ <http://blogs.crikey.com.au/rooted/2011/01/19/origin-of-the-north-atlanticfreeze/>

³⁰ Global Carbon Project. Canadell et al. 2006 GCTE-IGBP Book Series

³¹ Lovelock, J (2009), "The Vanishing Face of Gaia" (Basic Books)

circum-Antarctic, driving La Nina phases in the Pacific Ocean, may in part reflect such melt water pulses³².

VI. 21st century climate projections

Projections of 21st century climate trends suggest the climate is at a lag period tracking toward greenhouse Earth conditions such as existed when atmospheric CO₂ levels exceeded ~500±50 ppm, with intermediate stages reaching conditions as during Pliocene (~3 Ma) and Miocene (~16 Ma) peaks when temperatures were ~2°C to 4°C higher than pre-industrial Holocene levels.

A new IPCC-2011-AR5 draft report projecting extreme weather events³³ states: *"Models project substantial warming in temperature extremes by the end of the 21st century. It is virtually certain that increases in the frequency and magnitude of warm daily temperature extremes and decreases in cold extremes will occur in the 21st century on the global scale. It is very likely that the length, frequency and/or intensity of warm spells, or heat waves, will increase over most land areas. Based on the A1B and A2 emissions scenarios, a 1-in-20 year hottest day is likely to become a 1-in-2 year event by the end of the 21st century in most regions, except in the high latitudes of the Northern Hemisphere, where it is likely to become a 1-in-5 year event"*

The report further states: *"Low-probability high-impact changes associated with the crossing of poorly understood climate thresholds cannot be excluded, given the transient and complex nature of the climate"*, i.e. the likelihood of tipping points in the climate system is not considered. The report also states: *"projected climate extremes under different emissions scenarios generally do not strongly diverge in the coming two to three decades"*. It is possible that, at 392 ppm CO₂ and >460 ppm CO₂-e atmospheric GHG levels are as high as to trigger amplifying feedbacks, apart from further emission rises.

Estimates of climate projections for the 21st century and beyond need to take account of the following:

- A. The current Earth atmosphere energy balance—the difference between energy/heat absorbed by the from solar radiation and emitted back to space, is estimated at +3.2 Watt/m² relative to pre-industrial age conditions, equivalent to +2.3°C (IPCC-2007; Hansen et al., 2011), a consequence of rising GHG from fossil carbon emissions, land clearing and fires (Fig. 3).
- B. The +2.3°C rise relative to pre-industrial age is currently masked by the ~ -1.6 Watt/m² or ~ -1.1°C sulphur aerosol effect emitted from fossil fuel burning. The short atmospheric residence time of <3 years of SO₂ and derived sulphuric acid imply Earth is currently under an (unintended) sun-shielding geo-engineering regime whose removal would result in an abrupt temperature rise. The gradual temperature rise projections such as portrayed by the IPCC-AR4³⁴ do not betray the effect of sulphur aerosols, nor do they account for feedback effects such as the opening of the Arctic Ocean, ice sheet breakdown, methane release from permafrost and polar seas and lakes

³² <http://www.sciencedaily.com/releases/2011/09/110918144941.htm>

³³ IPCC SREX Summary for Policymakers. <http://ipcc-wg2.gov/SREX/>

³⁴ IPCC AR4 Summary for Policy Makers Figure SPM-5

- C. At a level of 392 ppm CO₂ and 455 ppm CO₂, the GHG at the rate of ~2 ppm CO₂ per year, surpassing rates recorded from the last 55 million years, threatens a tipping point which bears an analogy to the PETM (Palaeocene-Eocene Thermal Event)³⁵ and D-O³⁶ events referred to above. However, as the PETM was superposed on greenhouse Earth conditions some 6°C higher than background levels, under an atmosphere of ~4000 ppm CO₂, no direct analogy can be drawn with the Anthropocene. Likewise, D-O (Dansgaard-Oeschger) cycles were superposed on glacial conditions some ~ -5°C cooler than the Holocene, rendering comparisons inapplicable. Nonetheless, these events manifest a sensitivity of the atmosphere to moderate radiative forcing at levels at present approached by the atmosphere. Notably in each of the above events temperature rise reached or exceeded ≥4°C. This included thermal events driven by methane release or orbital forcing. Whereas the explanation for this degree of change is unknown, possibly it possible reflects the level of amplifying climate feedbacks from the ocean-land-biosphere system, including CO₂ release and ice melt/water interaction.
- D. The development of the ENSO cycle since the late Pliocene ~3.0 Ma, signifying cooling of the Earth and onset of polar-derived ocean currents which drive the La Nina phases, appears to be currently reversed through temporal increase in the frequency of El Nino phases (Fig. 14). This reversal constitutes a clear portent for advance of ENSO-free climate conditions leading to different terrestrial climates. Possibly the development of a strong La Nina phase since 2009 represents enhancement of the Humboldt and California current due to cold Antarctica and Arctic ice melt water.
- E. As the large ice sheets continue to melt transient cooling of sub-polar ocean regions may be expected, including a likely collapse of the North Atlantic Thermohaline Current, leading to abrupt cooling of Western Europe and North-east America. According to Hansen and Sato (2011) *"iceberg discharge rate temporarily overwhelms greenhouse warming, cooling high latitude atmosphere and ocean mixed layer below current levels."*
- F. Estimates of sea level rise depend on the melt rate of the Greenland and Antarctic ice sheets. According to the above authors the most reliable indication of the imminence of multi-meter sea level rise may be provided by empirical evaluation of the doubling time for ice sheet mass reported by Velicogna (2009)³⁷.

The history of the atmosphere-ocean-cryosphere system, portrayed in earlier sections, and the extreme rate of greenhouse gas rise in the atmosphere, militate for abrupt tipping points rather than smooth climatic transitions, a projection consistent with the current string of extreme weather events around the globe. As stated by Joachim Schellnhuber, director of the Potsdam Climate Impacts Institute: *"we're simply talking about the very life support system of this planet"*.

³⁵ Zachos et al., 2008

³⁶ Ganopolski and Rahmstorf, 2001

³⁷ Velicogna, I., 2009: Increasing rates of ice mass loss from the Greenland and Antarctic ice sheets revealed by GRACE, *Geophys. Res. Lett.*, 36, L19503, doi:10.1029/2009GL040222.

VII. CO₂ draw-down

The current rise in atmospheric CO₂ levels to 392 ppm and near 455 ppm CO₂-e at a rate of ~2 ppm CO₂ per year, unprecedented in recorded geologic history, is approaching conditions which existed on Earth in the mid-Miocene some 16 million years ago. Proposals for averting tipping points in the climate system include two main approaches: (A) solar shielding, and (B) CO₂ sequestration. Table 2 summarizes advantages and problems associated with principal proposed climate geo-engineering methods, suggesting none is likely to be effective, with the notable possible exception of attempts at draw-down of atmospheric CO₂.

It follows from the summary:

1. Stratospheric sulfur injections are both short-lived and destructive in terms of ocean acidification and retardation of the monsoon and of precipitation over large parts of the Earth, including Africa, southern and southeast Asia.
2. Retardation of solar radiation through space sunshades is of limited residence time, would not prevent ocean acidification from ongoing carbon emission, but could be used to gain time for application of CO₂ draw-down.
3. Dissemination of ocean iron filings and temperature exchange through pipe systems are likely ineffective in transporting CO₂ for storage in safe water depths.
4. CO₂ sequestration using soil carbon, biochar and possible chemical methods such as "sodium trees", combined with rapid decline in industrial CO₂ emissions, can in principle help slow down, and in future possibly even reverse, the current rise in atmospheric CO₂ toward mean global temperatures.
5. Budgets on a scale of military spending (>\$20 trillion since WWII) are required in any attempt to retard the current trend toward likely tipping points, likely to follow amplifying feedbacks of global warming, including the opening of the Arctic Ocean, melting of ice sheets, release of methane from permafrost and lakes and forest fires.

Top priority ought to be given to fast track testing of soil carbon burial/biochar methods, chemical ("sodium trees") and incentives for invention of new CO₂ sequestration methods. It is likely a species which placed a man on the moon can also develop effective CO₂ sequestration methods, but only if coordinated global efforts are made and suitable funding is provided.

Table 2.

Main proposed solar mitigation and atmospheric carbon sequestration methods

Method	Supposed advantages	Problems
SO ₂ injections	Cheap and rapid application	Short multi-year atmospheric residence time; ocean acidification; retardation of precipitation and of monsoons
Space sunshades/mirrors	Rapid application. No direct effect on ocean chemistry	Limited space residence time. Uncertain positioning in space. Does not mitigate ongoing acidification by emissions.
Ocean iron filing fertilization enhancing phytoplankton	CO ₂ sequestration	No evidence that dead phytoplankton would not release CO ₂ back to the ocean surface.
Ocean pipe system for vertical circulation of cold water to enhance CO ₂ sequestration	CO ₂ sequestration	No evidence the cold water would circulate back to ocean depths where CO ₂ is prevented from returning to the surface.
“Sodium trees” - NaOH liquid in pipe system sequestering CO ₂ to Na ₂ CO ₃ , separation and burial of CO ₂ .	CO ₂ sequestration, estimated by Hansen et al. (2008) at ~\$300 per ton CO ₂	Unproven efficiency; need for CO ₂ burial; \$trillions expense (though no more than current military expenses).
Soil carbon burial/biochar	Effective means of controlling the carbon cycle (plants+ soil exchange with the atmosphere)	Requires a huge international effort by a workforce of millions of farmers
serpentine CO ₂ sequestration	CO ₂ sequestration	Possible scale unknown

VIII. 2011 Climate developments³⁸

The combined global land and ocean average surface temperature for September 2011 was the eighth warmest on record at 15.53°C (59.95°F), which is (0.53°C) 0.95°F above the 20th century average of 15.0°C (59.0°F). The margin of error associated with this temperature is +/- 0.11°C (0.20°F).

Separately, the global land surface temperature was 0.87°C (1.57°F) above the 20th century average of 12.0°C (53.6°F), making this the fourth warmest September on record. The margin of error is +/- 0.24°C (0.43°F).

The September global ocean surface temperature was 0.40°C (0.72°F) above the 20th century average of 16.2°C (61.1°F), making it the 14th warmest September on record. The margin of error is +/- 0.04°C (0.07°F).

The combined global land and ocean average surface temperature for the January – September period was 0.51°C (0.92°F) above the 20th century average of 14.1°C (57.5°F), making it the 11th warmest such period on record. The margin of error is +/- 0.10°C (0.18°F).

The January – September worldwide land surface temperature was 0.80°C (1.44°F) above the 20th century average — the 7th warmest such period on record. The margin of error is +/- 0.20°C (0.36°F). The global ocean surface temperature for the year to date was 0.41°C (0.74°F) above the 20th century average and was the 12th warmest such period on record. The margin of error is +/- 0.04°C (0.07°F).

A warm December season is forecast for Australia, with warmer days more likely over the northern tropics and southern Australia and warmer nights more likely over large parts of the continent, with the strongest odds in the northeast and southwest. The main driver behind this outlook is the persistence of above average temperatures across the central to south-eastern Indian Ocean. A wetter season is forecast for northern Australia

http://www.bom.gov.au/climate/ahead/temps_ahead.shtml

http://www.bom.gov.au/climate/ahead/rain_ahead.shtml

³⁸ <http://www.ncdc.noaa.gov/sotc/global/2011/9>.

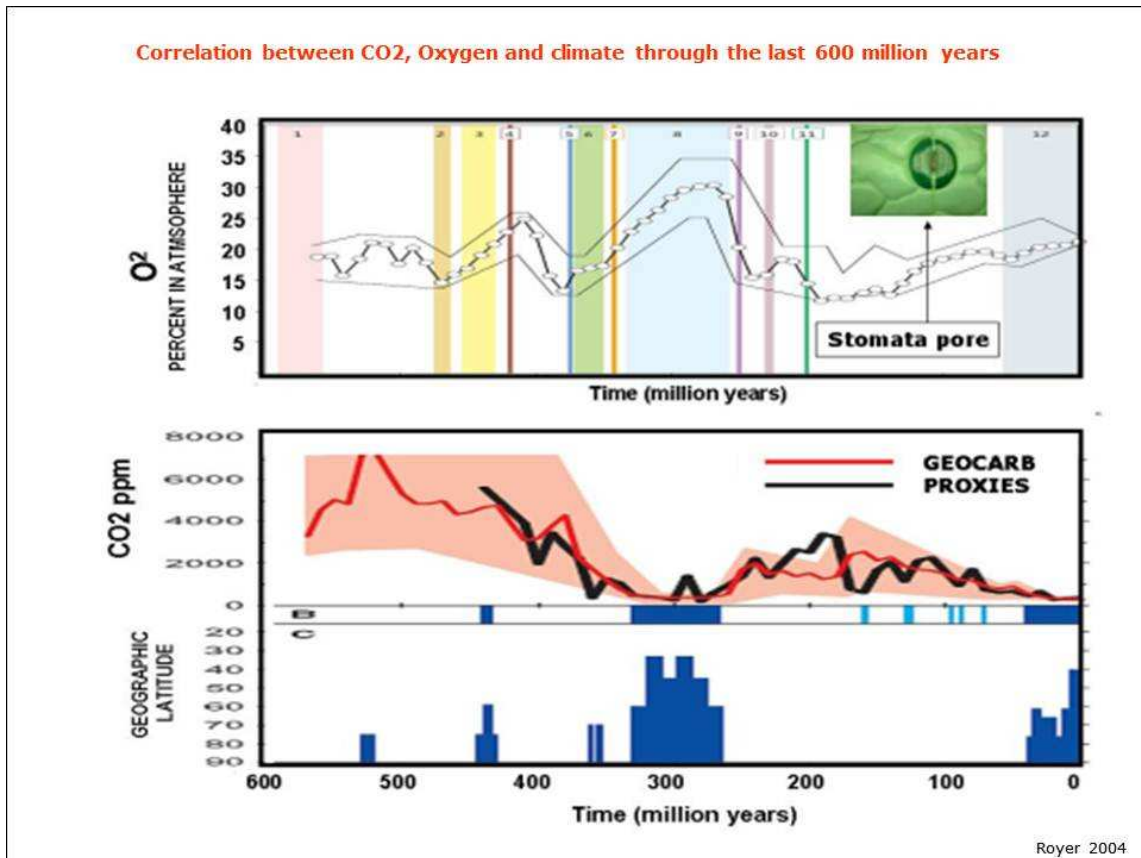


Figure 1.

Evolution of atmospheric CO₂ and oxygen with time. **(A)** Details of CO₂ proxy data for the Phanerozoic (540 Ma to the present). Five-point running averages of individual proxies (fossil plant pores [stomata], nitrogen minerals, carbon isotopes and GEOCARB III comparison). Black curve represents average values in 10 my time-steps. Blue histograms represent duration and intensity of glacial periods (Royer et al., 2004); **(B)** Evolution of atmospheric oxygen with time (Berner et al., 2007).

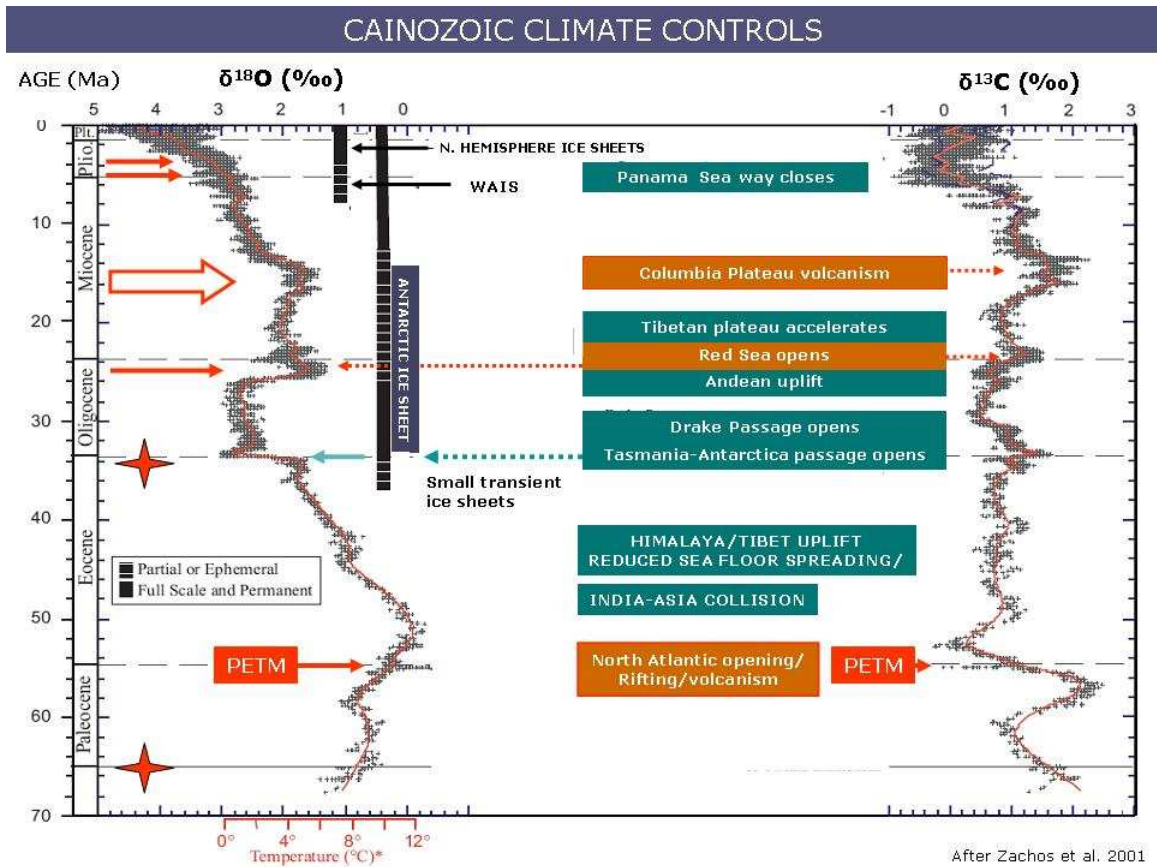


Figure 2.

Climatic variations from 65 Ma based on global deep-sea oxygen and carbon isotope records compiled from more than 40 DSDP and ODP sites (Zachos et al., 2001). Note the sharp descent into ice age conditions at c.34 Ma, when CO₂ levels declined below 500±50 ppm, the mild warming during the late Oligocene and mid-Miocene, and the sharp decline in temperatures during the Pliocene and Pleistocene.

**Global temperatures relative to peak Holocene and Pliocene temperatures
Hansen and Sato 2011**

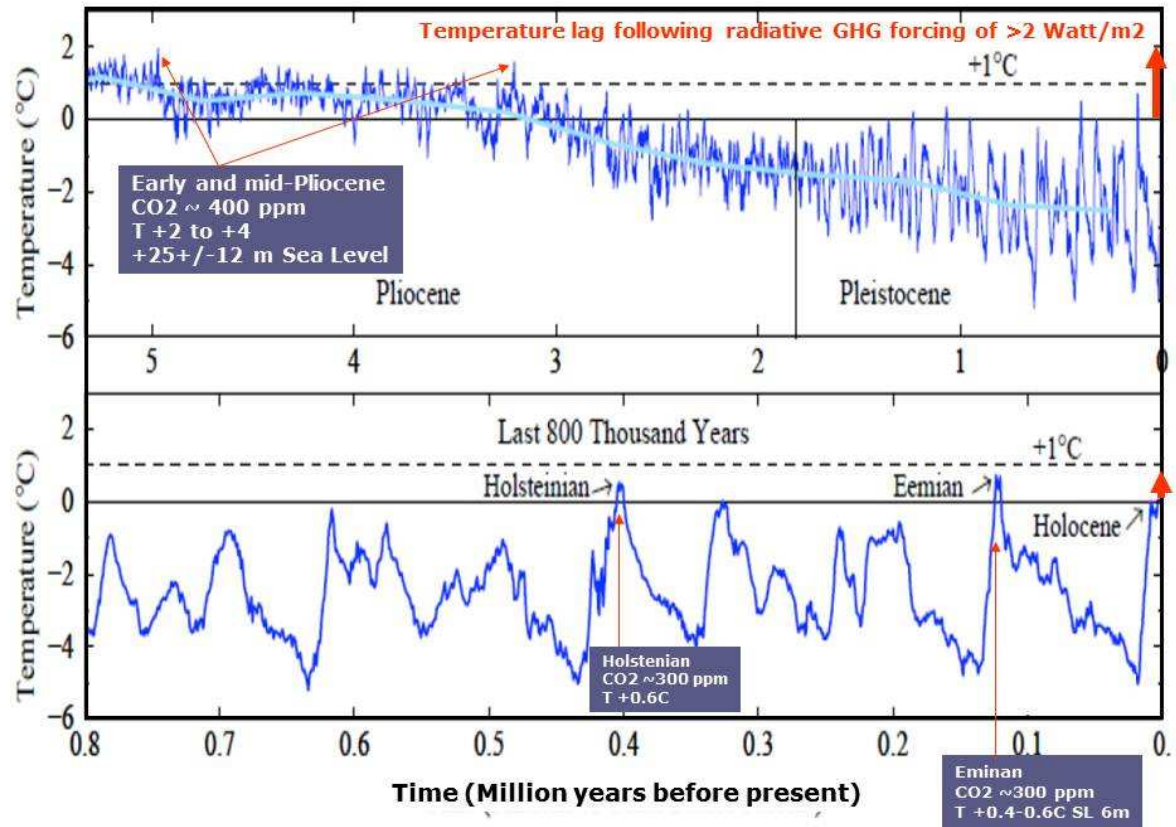


Figure 3.

Global temperatures relative to peak Holocene and Pliocene temperatures (from Hansen and Sato, 2011).

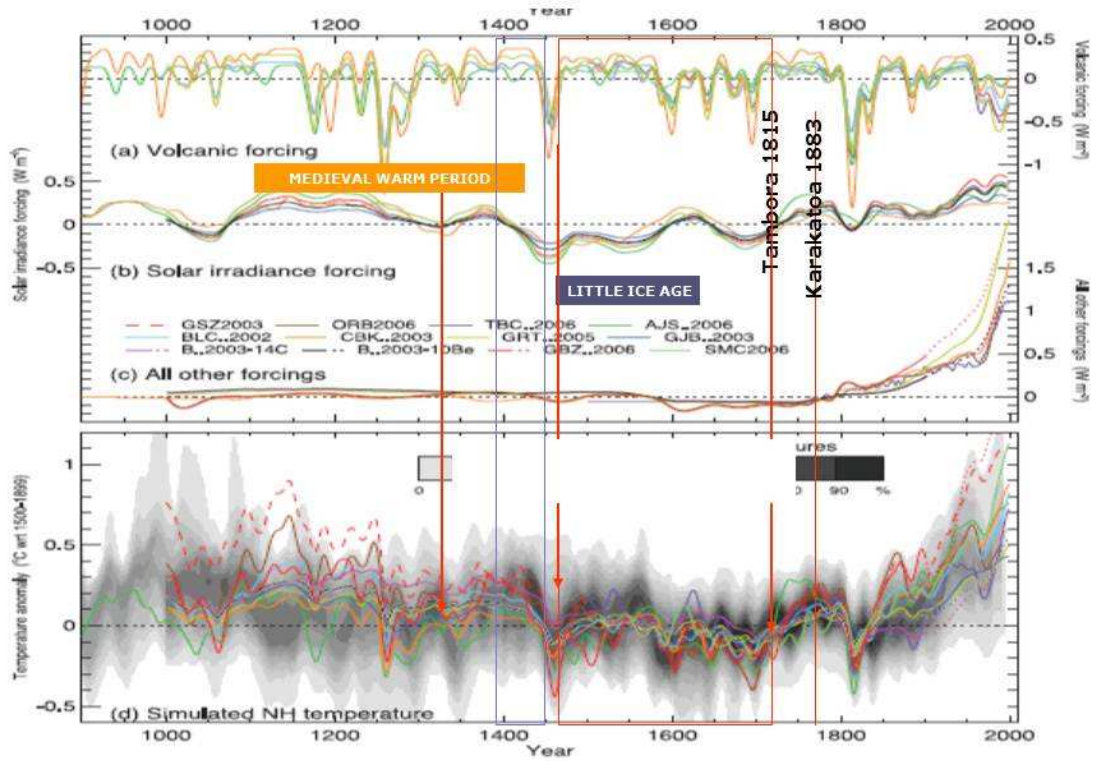


Figure 4.

Radiative forcing and proxy-based temperatures during the last 1.1 kyr (IPCC-2007 Chapter 4: Palaeoclimate, Fig. 6.13).

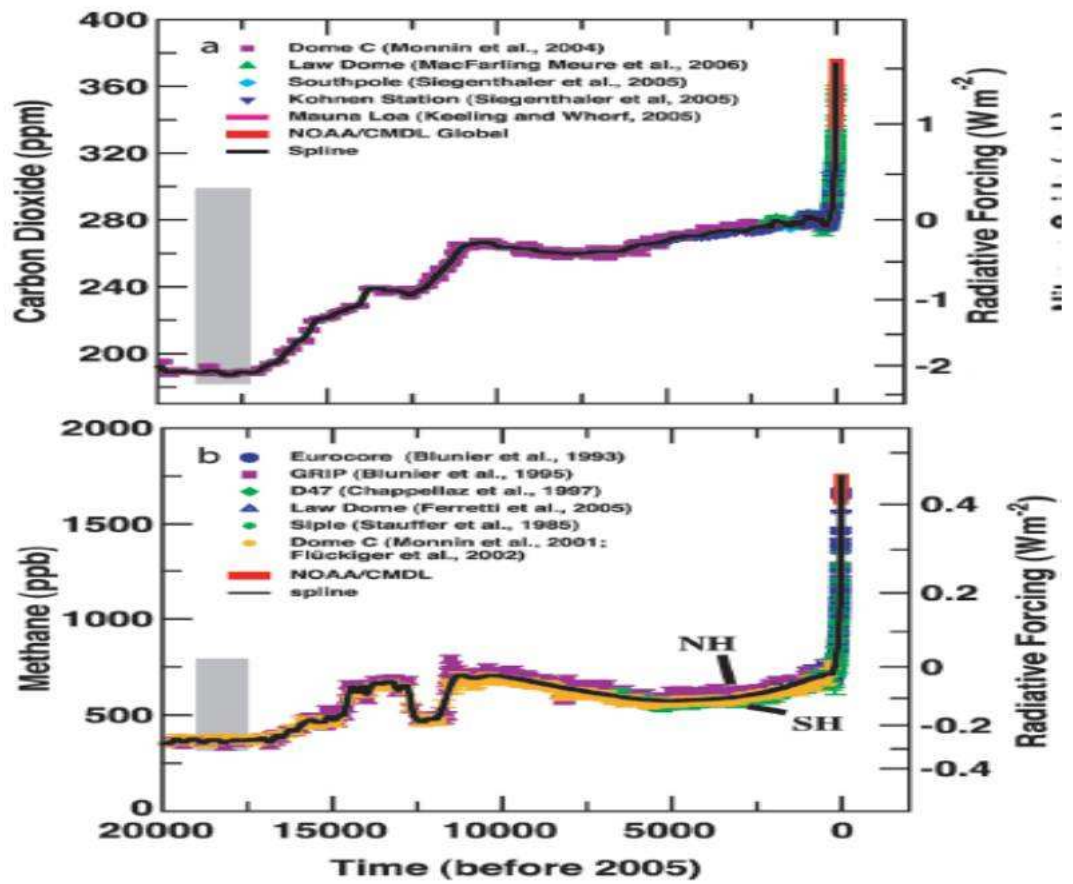


Figure 5.

Radiative forcing for the period 20 kyr onward correlated with (a) carbon dioxide (CO₂); (b) methane (CH₄). IPCC-2007 AR4 Figure TS.2:

Human perturbation of the global carbon budget

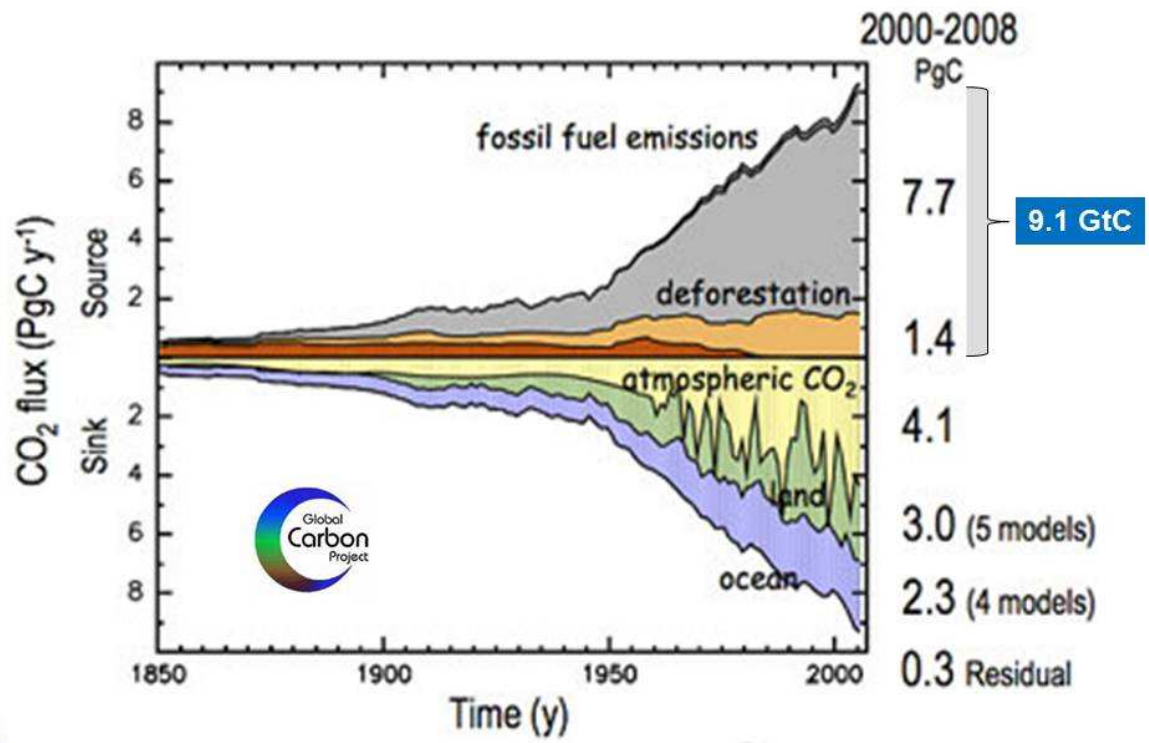
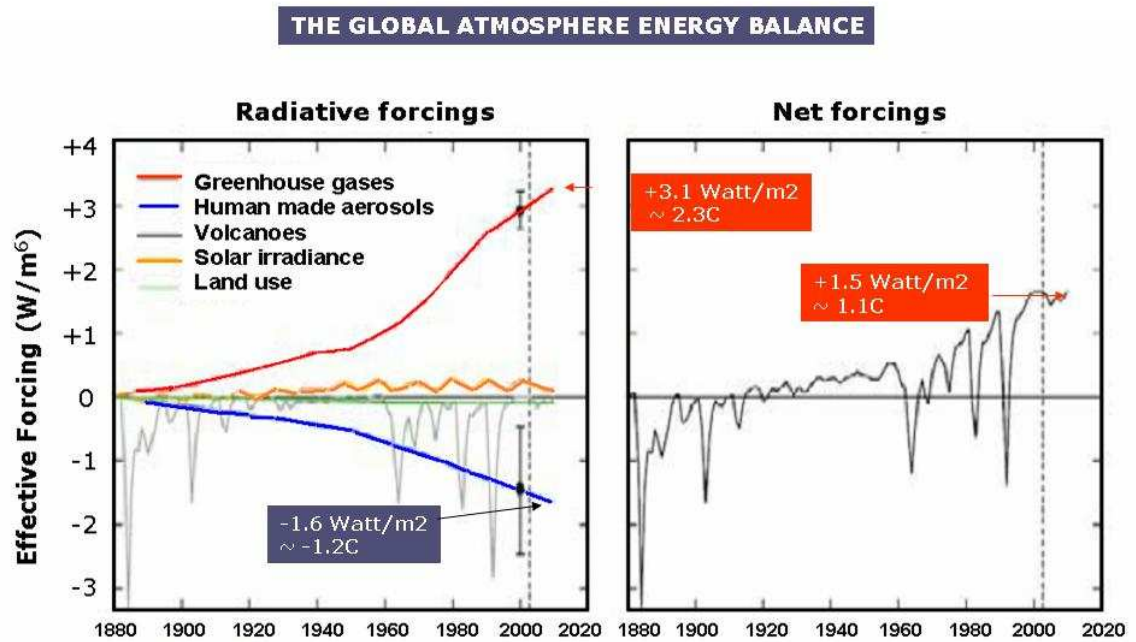


Figure 6.

Fractionation of human emitted CO₂ since 1850 between the atmosphere, oceans and vegetation. Global Carbon Project.



Hansen et al. 2011

Figure 7.

- (A) Development of radiative forcing 1880-2010 in terms of energy changes of greenhouse gases (CO₂, CH₄, N₂O, O₃), human emitted aerosols (mainly SO₂), volcanic eruptions, solar radiation and land use.
- (B) Net variations in global energy levels (based on A). Hansen et al. 2011.
http://www.columbia.edu/~jeh1/mailings/2011/20110415_EnergyImbalancePaper.pdf

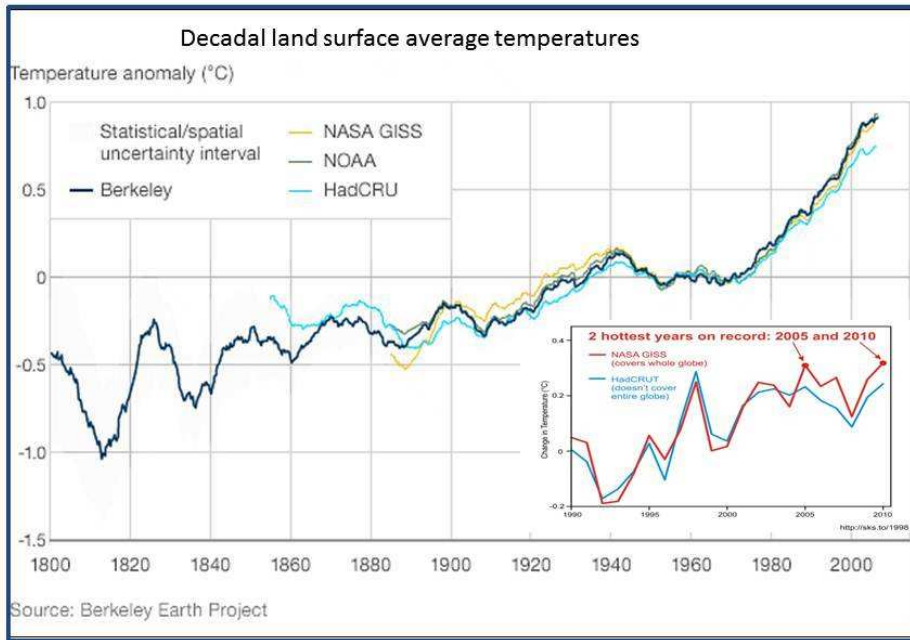


Figure 8A.

Decadal land surface average temperatures including data by NASA/GISS, NOAA, HadCRU and the Berkley Earth Project. Inset shows data for 1990-2010 from NASA/GISS and HadCRUT, including peak temperatures for 2005 and 2010.

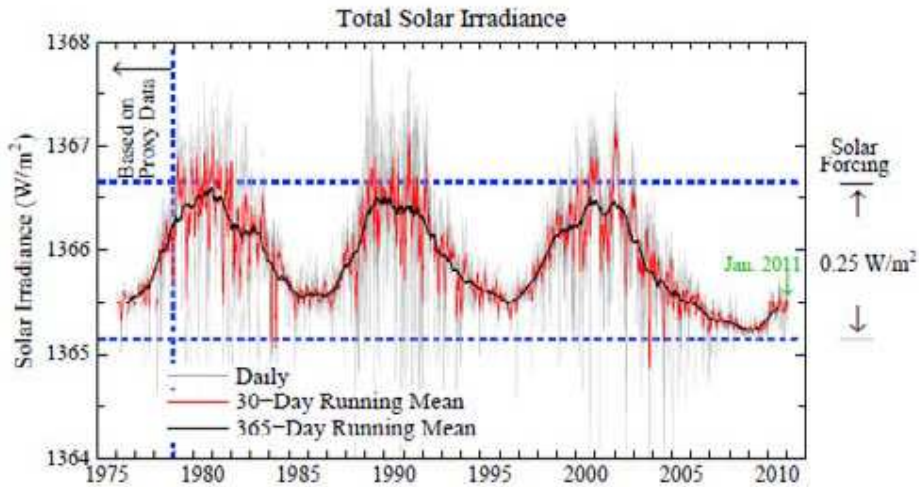


Figure 8B

Solar irradiance from composite of several satellite-measured time series Frohlich and Lean, 1998. Geophys. Res. Let., 25, 4377-4380, 1998.

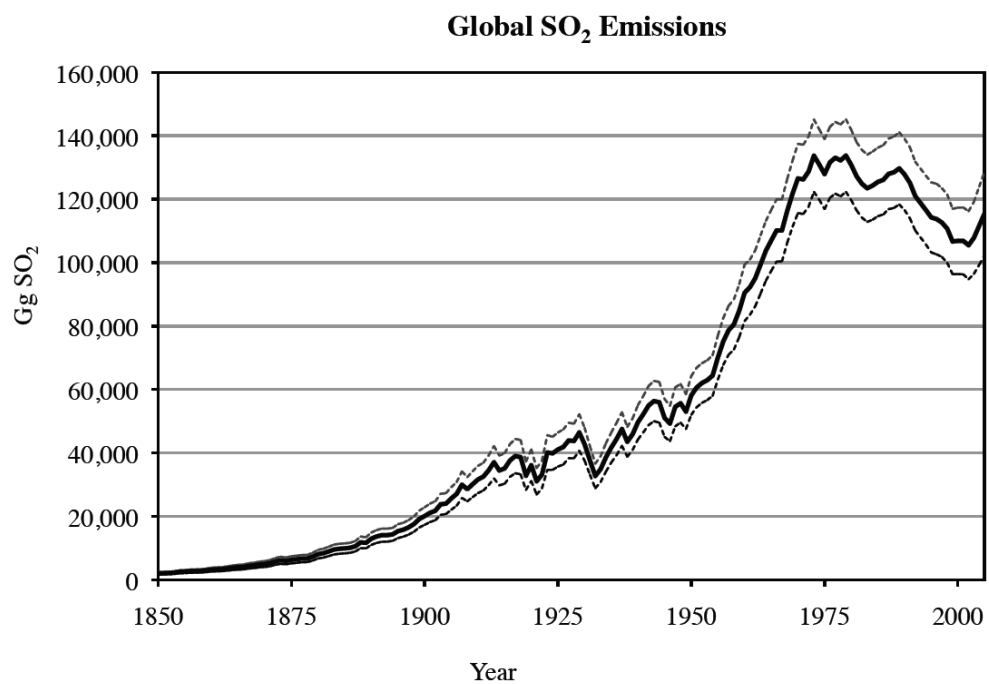


Figure 8C.

Global sulphur dioxide emissions from fuel combustion and process emissions with central value (solid line) and upper and lower uncertainty bounds (dotted lines). Anthropogenic sulphur dioxide emissions: 1850–2005. Smith et al., 2011. *Atmos. Chem. Phys.*, 11, 1101–1116.

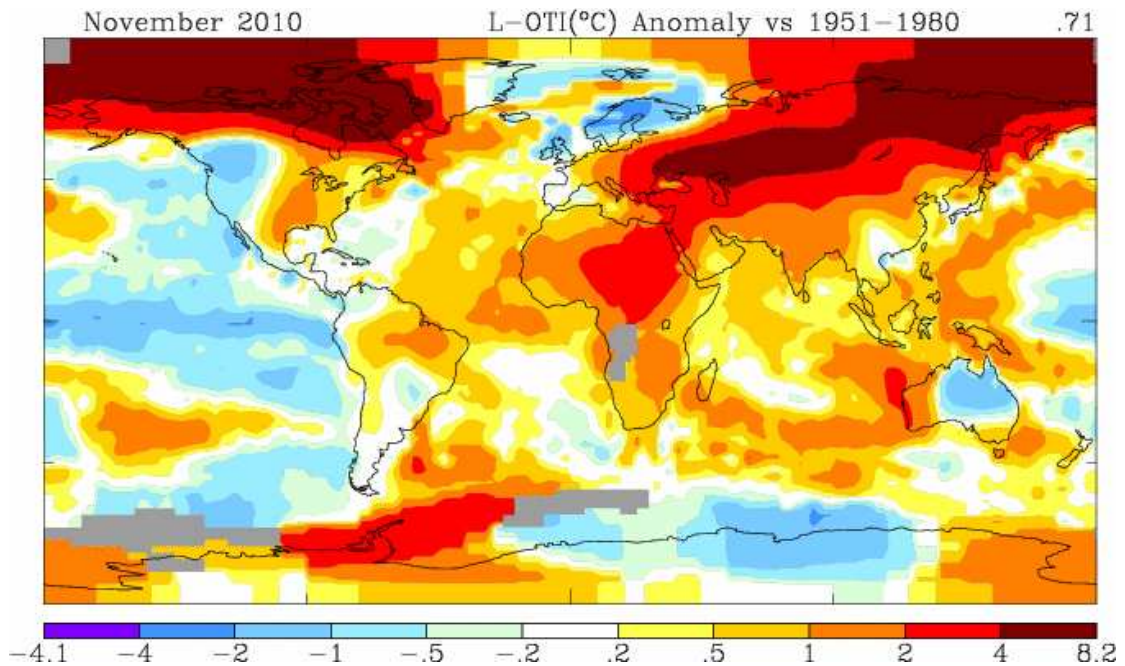


Figure 9.

Global temperature anomalies for November 2010 relative to the 1951-1980 baseline. Winter temperature increase of up to 4 degrees C over Siberia and Canada are contrasted with cold North Atlantic temperatures, representing flow of cold vapour-rich air from the relatively ice-free Arctic Sea which led to snow storms over NE North America and western Europe. NASA/GISS. <http://data.giss.nasa.gov/gistemp/graphs/>

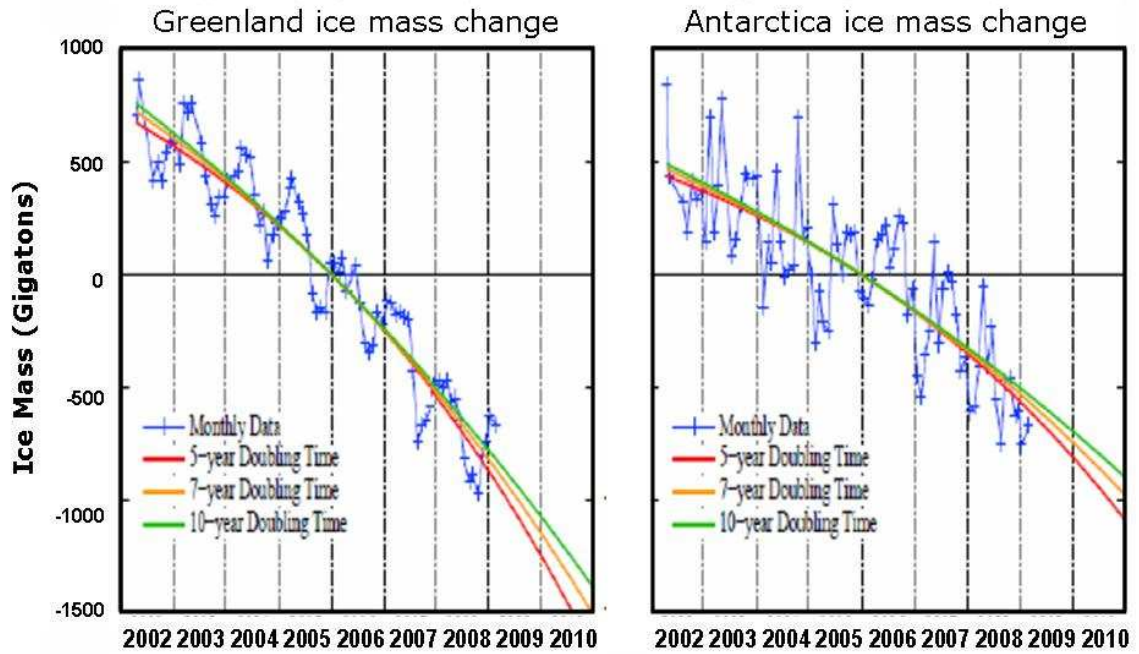


Figure 10.

Decadal, annual and seasonal changes in ice masses in Greenland and Antarctica from gravitational field measurements by Velicogna (2009) (Hansen and Sato, 2011). <http://www.agu.org/pubs/crossref/2011/2011GL046583.shtml>

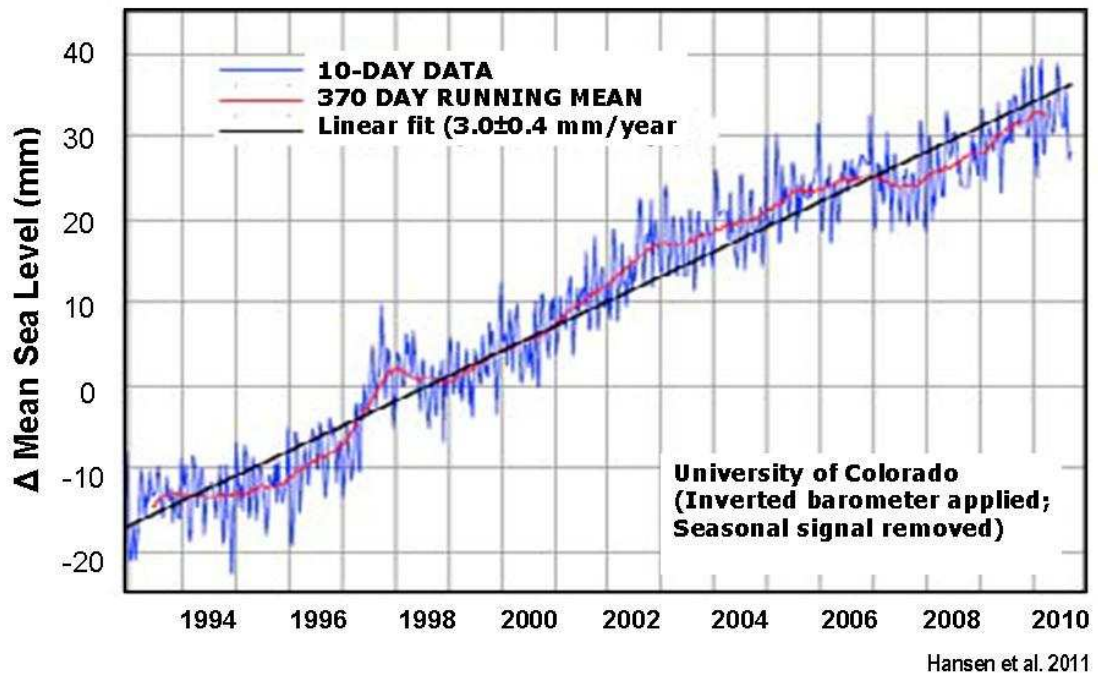


Figure 11.

Mean sea level rise between 1993-2010 in terms of 10-days data, 370 days running mean and a linear fit, based on satellite altimeter measurements calibrated with tide-gauge measurements (Nerem et al., 2006). University of Colorado. After Hansen et al. 2011.
http://www.columbia.edu/~jeh1/mailings/2011/20110415_EnergyImbalancePaper.pdf

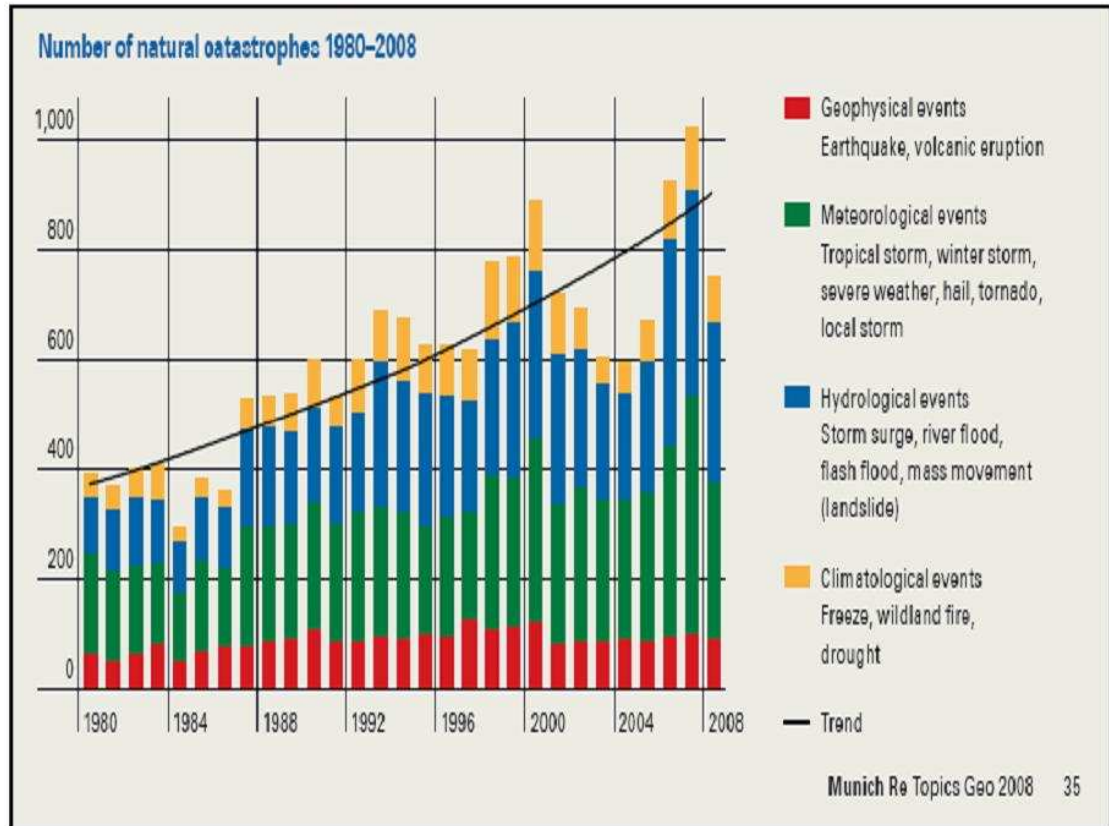


Figure 12.

Frequency of global extreme weather events and geophysical events, 1998 - 008. From Topics Geo: Natural catastrophes 2008 analyses, assessments and positions.

<https://www.munichre.com/touch/login/en/service/login.aspx?ReturnUrl=/touch/publications/en/list/default.aspx?id=1060>

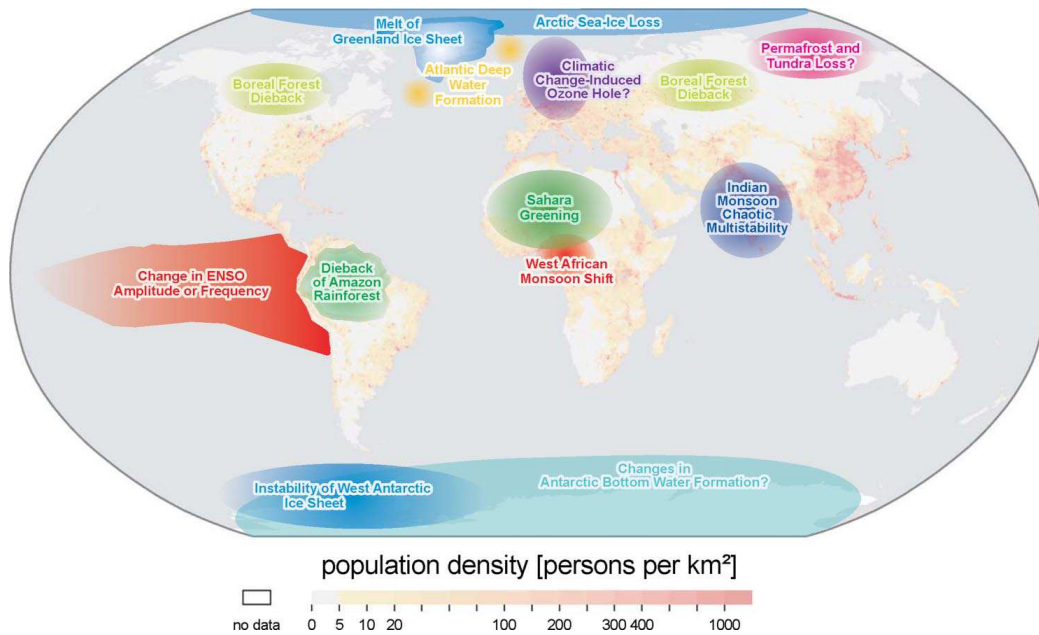


Figure 13.

Map of potential policy-relevant tipping elements in the climate system, updated from ref. 5 and overlain on global population density. Subsystems indicated could exhibit threshold-type behaviour in response to anthropogenic climate forcing, where a small perturbation at a critical point qualitatively alters the future fate of the system. They could be triggered this century and would undergo a qualitative change within this millennium. We exclude from the map systems in which any threshold appears inaccessible this century (e.g., East Antarctic Ice Sheet) or the qualitative change would appear beyond this millennium (e.g., marine methane hydrates). Question marks indicate systems whose status as tipping elements is particularly uncertain.

Pliocene 5.3 – 2.8 Ma: Evolution of the ENSO

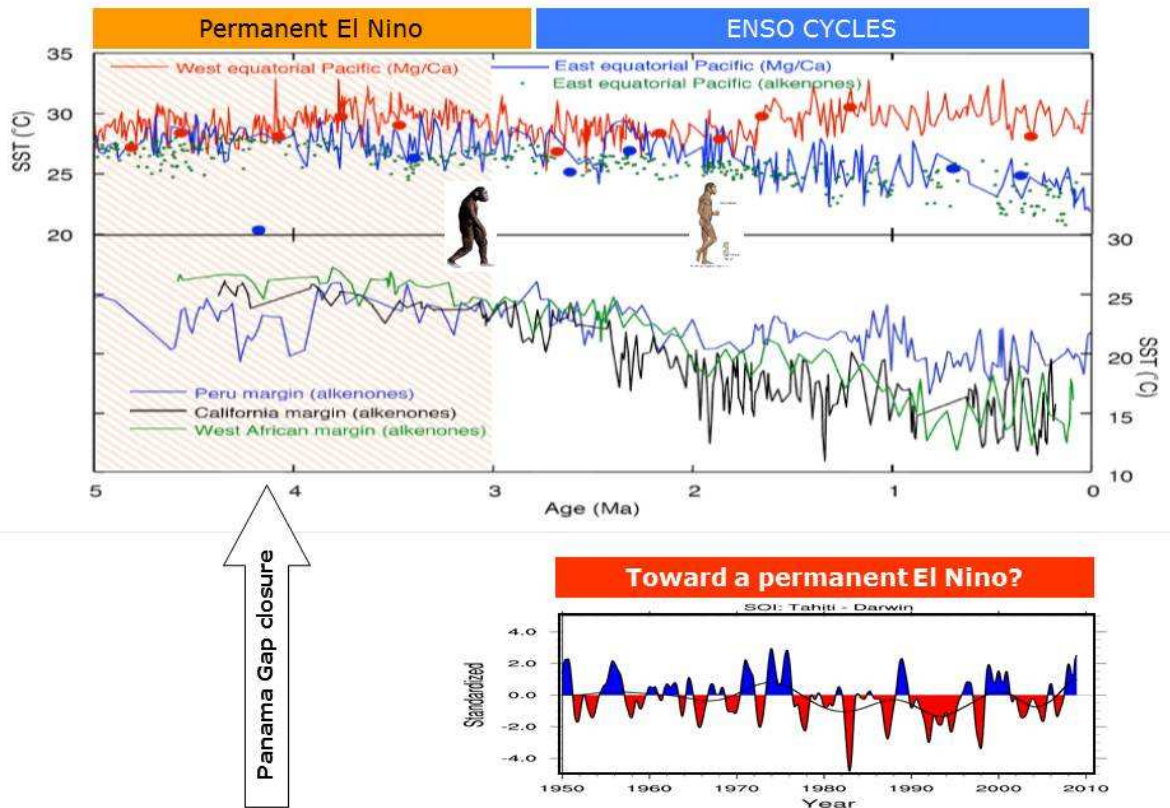


Figure 14.

- (A) Evolution of the ENSO cycle from the Pliocene (5 – 2.8 Ma) through the Pleistocene (2.8 Ma to 0.01 Ma), displaying increased temperature polarity across the Pacific Ocean with time.
<http://www.sciencemag.org/content/312/5779/1485>
- (B) The Southern Oscillation Index between 1950-2008, showing increased prevalence of the El Nino phase
http://gcmd.nasa.gov/records/GCMD_NOAA_NWS_CPC_SOI.html